

Article

Development of Radiator with Thermoplastic Polymer and Insert-Molded Aluminum Alloy Parts for Light-Emitting Diode Headlights

Yenlung Chen ¹, Juikun Chang ^{2,3}, Chun Huang ⁴, Changche Chiu ⁵, Wei Lai ⁵, Zhiting Ye ^{5,*}  and Pin Han ^{1,*} 

- ¹ Graduate Institute of Precision Engineering, National Chung Hsing University, No. 145, Xingda Rd., South Dist., Taichung 402, Taiwan; d105067001@mail.nchu.edu.tw
- ² R&D Center, Dayei Precise Technology Co., Ltd., No. 20, Ln. 372, Kinmen St., Banqiao Dist., New Taipei City 22071, Taiwan; 0812alu@gmail.com
- ³ R&D Center, PUZI Enterprise Co., Ltd., No. 20, Ln. 372, Kinmen St., Banqiao Dist., New Taipei City 22071, Taiwan
- ⁴ R&D Center, Nytex Composites Co., Ltd., 17F., No. 94, Sec. 1, Sintai 5th Rd., Sijhih Dist., New Taipei City 221, Taiwan; jim@nytex.com
- ⁵ Department of Mechanical Engineering, Advanced Institute of Manufacturing with High Tech Innovations, National Chung Cheng University, 168, University Rd., Min Hsiung, Chiayi 62102, Taiwan; g10421033@ccu.edu.tw (C.C.); william19961758@gmail.com (W.L.)
- * Correspondence: imezty@ccu.edu.tw (Z.Y.); pin@dragon.nchu.edu.tw (P.H.)

Abstract: The increasing popularity of electric vehicles has increased the demand for lightweight auto parts. However, the excessive weight of traditional metal heat sinks has remained a concern. Metal has excellent thermal conductivity but low radiation efficiency. Conversely, thermoplastic polymers have excellent heat radiation efficiency but poor thermal conductivity. In this study, we propose a radiator constructed using thermoplastic polymer and insert-molded aluminum alloy parts to maintain the low junction temperature of light-emitting diodes (LEDs); the radiator's weight is reduced through a combination of aluminum alloy and a thermally conductive polymer designed for automotive headlights. At an LED thermal load of 11.48 W, the measured temperature on the LED pad is 60.8 °C. The weight of the proposed radiator is 23.37% lighter than that of a pure metal radiator. When the lightweight radiator is used in high-power LED headlights, it effectively dissipates heat within a limited space.

Keywords: LED headlight; thermal conductivity; thermoplastic polymer; aluminum alloy; composite radiator



Citation: Chen, Y.; Chang, J.; Huang, C.; Chiu, C.; Lai, W.; Ye, Z.; Han, P. Development of Radiator with Thermoplastic Polymer and Insert-Molded Aluminum Alloy Parts for Light-Emitting Diode Headlights. *Appl. Sci.* **2022**, *12*, 5385. <https://doi.org/10.3390/app12115385>

Academic Editor: Andrés Márquez

Received: 14 April 2022

Accepted: 25 May 2022

Published: 26 May 2022

Publisher's Note: MDPI stays neutral with regard to jurisdictional claims in published maps and institutional affiliations.



Copyright: © 2022 by the authors. Licensee MDPI, Basel, Switzerland. This article is an open access article distributed under the terms and conditions of the Creative Commons Attribution (CC BY) license (<https://creativecommons.org/licenses/by/4.0/>).

1. Introduction

The increased focus on energy efficiency has prompted the continual introduction of new light-emitting diode (LED) applications with ever expanding scopes. LED headlights are expected to completely replace energy-intensive car lights over time. With the evolution of automotive technology, the application of high-power, high-brightness LEDs in the vehicle headlight market has attracted considerable attention, especially in the electric vehicle market; however, battery life remains a major limiting factor [1–5]. At a given current, the luminous intensity of white light is approximately 180 lm/W, which is considerably higher than that of traditional light sources. The current–voltage characteristics of traditional light sources and LEDs are substantially different, but these technologies can be compared using the same power input [6].

Compared with traditional light sources, LEDs have numerous advantages, such as environmentally friendly properties, high reliability, high efficiency, and a long life [7,8]. Studies on LED lighting have focused on application-specific LED packaging, whose volume and size can be as small as one-eighth of that of traditional LEDs. The life cycle

impact of LED products is still not completely understood. As of 2022, phosphors, silicones, epoxies, and LEDs are still typically sent to landfills [9–11]. However, a major problem that reduces the lifetime of an LED system is the heating generated by the system itself [12–14]. A high LED junction temperature accelerates the degradation of the packaging material of an LED, which weakens the LED and causes phenomena such as yellowing, cracking, and delamination of encapsulation materials [15,16].

When the junction temperature of an LED increases, its life is considerably shortened. Researchers have conducted parameter analyses to optimize the thermal model of a new type of heat sink that is suitable for LED lamps [17]. Kilic et al. proposed a novel design that uses a liquid-cooled heat sink to cool electronic equipment; in this manner, the uniform temperature distribution is achieved [18]. Shuo et al. conducted a finite element analysis by applying a thermal resistance network model in a three-dimensional environment, changing thermal stress distribution, thereby demonstrating the performance of analyzing LED thrust under high-temperature conditions [19]. Electronic cool systems often utilize a plate-fin heat sink [20]. Hamdi proposed the application of numerical methods for assessing the influence of orientation on a heat sink that was utilized to cool an LED light [21]; in that study, cooling performance was evaluated using a ribbed flat-plate fin heat sink. Abdelmlek et al. examined the thermal interaction between the leading array and placement design in natural convection by applying the computational fluid dynamics method [22]. Cenci et al. conducted a detailed examination of the recycling potential of the metals found in lighting products [23] and verified that the metals within LED lighting products are a major source of environmental pollution. Aluminum heat sinks also contribute considerably to the generation of hazardous waste [24]. Tang et al. proposed a novel design for a heat pipe-assisted compact heat sink for LEDs to reduce the junction temperature of LEDs [25]. Sevilgen et al. assessed the thermal and hydraulic performance of a novel LED cooling block with a dual-separated liquid cooling channel by testing it in cooling applications for single-LED and multi-LED printed circuit boards that are utilized in automotive lighting systems [26]. Mraz et al. experimentally evaluated the thermal performance of small liquid cooling systems that use polymeric hollow fibers and are designed to cool automotive lighting components that are integrated with high-power LEDs [27]. LED manufacturers are increasingly prioritizing the heat dissipation efficiency of LED light modules and reducing the mass of aluminum required in lighting products. Numerous factors determine the lifespan of an LED. The factors that increase the life of an LED system should be considered during an LED product development process [28,29].

In large vehicle headlights, an aluminum radiator is used to dissipate heat. Although high-power LED lights are widely used in the automotive industry, their heat dissipation efficiency is generally low, which results in high LED operating temperatures [30]. LED systems also provide benefits pertaining to human factors; for example, they can increase peripheral visual performance by reducing glare, thereby increasing customer demand for such lights. The design of headlight low beams must comply with the ECE R112 regulation [31,32]. Another notable point is that the optical design of headlights can potentially be applied to other light sources because the dimensions of an LED die are considerably smaller than those of a conventional light source [33–35]. With the advancement of technology, LED headlights can now provide partial shading, such that a direct LED light is less astigmatic; furthermore, road conditions can now be detected at all times through a sensing module, thus providing drivers with optimal and safe lighting in any driving environment [36]. Few studies have explored the design and use of heat sinks with thermoplastic polymer and insert-molded aluminum alloy parts. Thus, we propose a radiator with a thermoplastic polymer and insert-molded aluminum alloy parts to increase the heat transfer efficiency of an LED multichip module; we employ a combination of aluminum alloy and a thermally conductive polymer designed for automotive headlights to maintain the low junction temperature and lightweight property of the proposed LED.

2. Materials and Methods

The three modes of heat transfer are conduction, convection, and radiation. In accordance with the theory of heat conduction, the heat transfer process of LED lamps can be expressed as follows [37,38]:

$$\partial x \left(k_x \frac{\partial T}{\partial x} \right) + \partial y \left(k_y \frac{\partial T}{\partial y} \right) + \partial z \left(k_z \frac{\partial T}{\partial z} \right) + Q = 0 \quad (1)$$

where T is the temperature; Q is the heat source generated in the chip; region (R) represents the boundaries that are in contact with the ambient environment; and k_x , k_y , and k_z represent the thermal conductivity in the x , y , and z directions. At the boundaries, region R undergoes convection in an ambient environment, and this heat transfer process can be expressed as follows:

$$k_x \frac{\partial T}{\partial x} n_x + k_y \frac{\partial T}{\partial y} n_y + k_z \frac{\partial T}{\partial z} n_z = h(T_s - T_\infty) \quad (2)$$

where h is the convection heat transfer coefficient, T_s is the surface temperature, and n represents the outward normal in the x , y , and z directions [39].

For radiation, the surface-to-surface model is used, and the governing equation for this process is as follows:

$$Q_{rad} = \sigma \varepsilon_i F A_i (T_1^4 - T_2^4) \quad (3)$$

where Q is the heat transfer per unit time (W), rad is radiation, σ is the Stefan Boltzmann constant (W/m^2K^4), ε_i is the emissivity coefficient of the object, F is the effective radiation view factor, A_i is the surface area (m^2), and T_2 and T_1 represent the surface temperature and ambient temperature, respectively ($^\circ C$) [40].

The junction temperature T_j of the LED calculation method is obtained using the following equation:

$$T_j = T_s + P_{heat} * R_{th JS real} \quad (4)$$

where T_j is the junction temperature of the LED ($^\circ C$), T_s is the solder pad temperature ($^\circ C$), P_{heat} is the heating power (W), and $R_{th JS real}$ is the thermal resistance from the junction to the T_s measurement point of the LED ($^\circ C/W$).

Metals have greater heat conductivity than do thermally conductive plastic material, but the emissivity coefficient of thermally conductive plastic materials is higher to that of metals. Objects with temperatures that are higher than absolute zero can generate radiant heat. A higher temperature indicates that more energy is radiated. The basic material of the thermoplastic polymer CM-5000 (Nytex, Changhua County, Taiwan) is nylon, which has a thermal conductivity of $7 W/m \cdot K$, relative thermal index of $140^\circ C$, surface resistance of 10^5 , thermal emissivity coefficient of 0.92 , and flammability level of UL94-V0. The material of the aluminum alloy (AA1050) has a thermal conductivity coefficient of $180 W/m \cdot K$. In this study, we combined the high thermal conductivity characteristics of aluminum alloy with the high emissivity characteristics of thermoplastic polymer to develop an optimally designed lightweight radiator with high-efficiency heat sinks.

2.1. Structure of Composite Radiator

Figure 1 illustrates the structure of the proposed LED headlight radiator. Figure 1a is an illustration of a traditional LED headlight radiator that is shaped using aluminum alloy or other metals. Figure 1b shows a composite radiator with thermoplastic polymer and insert-molded aluminum alloy parts.

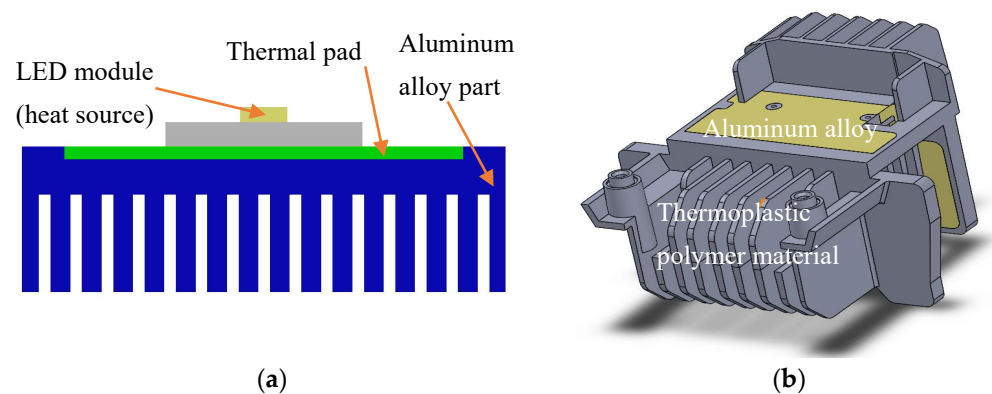


Figure 1. Basic structure of LED headlight radiator: (a) traditional LED headlight radiator and (b) composite radiator.

Figure 2 shows the dimensions of the thermoplastic polymer part. Its dimension is shown using a three-view format in Figure 2. Figure 2a–c shows the thermoplastic polymer part’s front, top, and side views, respectively; its width, length, and height are 103.2, 111, and 66.2 mm and its weight is 131 g.

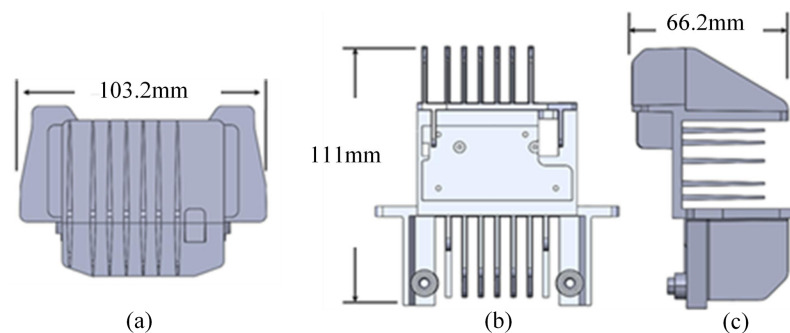


Figure 2. Thermoplastic polymer part: (a) front view, (b) top view, and (c) side view.

Figure 3 presents the dimensions of the aluminum alloy part. Figure 3a–c shows the front, top, and side views, respectively. The material of the aluminum alloy (AA1050) means it can effectively conduct the heat generated by the LED module used in the present study. Therefore, the aluminum alloy part was designed to be in direct contact with the LED module. The heat generated by the LED module was quickly and evenly conducted to the thermally conductive plastic through the aluminum alloy. The dimensions of the aluminum alloy part are shown using a three-view format in Figure 3; its width, height, and length are 42, 80, and 47 mm, respectively, and its gross weight is 56 g.

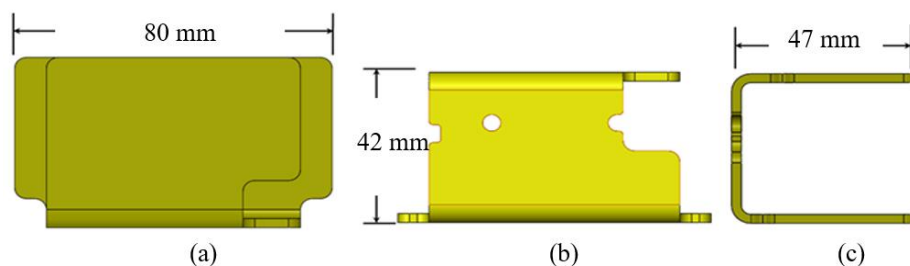


Figure 3. Aluminum alloy part: (a) front view, (b) top view, and (c) side view.

As indicated in Table 1, the weight of the composite headlight radiator is 187 g, which comprises the 56 and 131 g contributed by the aluminum alloy part and thermoplastic polymer part, respectively. The weight of the pure aluminum alloy headlight radiator is

244 g. The composite headlight radiator is approximately 57 g (23.37%) lighter than a pure aluminum alloy radiator.

Table 1. Weight comparison of the composite radiator and pure aluminum alloy radiator.

Material	Thermoplastic Polymer Insert Molding Aluminum Alloy	Pure Aluminum Alloy
Aluminum Alloy Part	56 g	244 g
Thermoplastic Polymer Part	131 g	-
Gross Weight	187 g	244 g
Weight percentage (%)	76.63%	100%

Therefore, the heat generated by the LED module can be quickly and uniformly transferred through the aluminum alloy body with a high heat transfer coefficient, after which the heat is dissipated into the air through the conductive plastic, which has a high emissivity coefficient. This process represents the final heat dissipation mechanism of the system.

2.2. Thermal Analysis and Optimization Simulation Design

Figure 4 illustrates the recommended design for the LED headlight radiator with thermoplastic polymer and insert-molded aluminum alloy parts; the cases of the thermoplastic polymer, aluminum alloy part, and LED module can be seen in the figure.

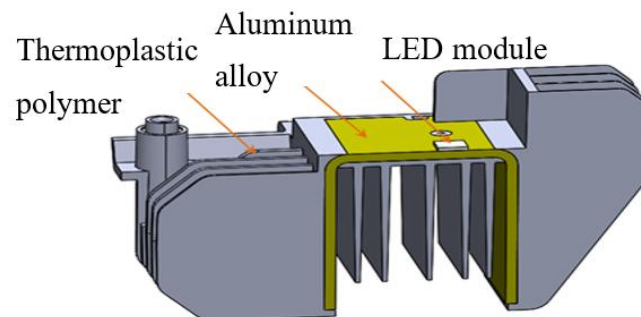


Figure 4. Radiator with thermoplastic polymer and insert-molded aluminum alloy parts.

Figure 5 presents the design of the composite radiator for LED headlights. Figure 5a shows the front view of the radiator; the thermoplastic polymer consists of multiple fins, which serve to increase its surface area for improved heat radiation. Figure 5b reveals the side view of the radiator; in addition to the fins on the Z-axis, several fins can also be observed on the X-axis, and they all serve to increase the surface area of the thermoplastic polymer. Figure 5c illustrates the top view of the radiator; the figure shows that the LED module is located at the top of the aluminum alloy and that the aluminum alloy is assembled on the thermoplastic polymer. Figure 5d presents the isometric view of the radiator, and it illustrates the assembly of the composite radiator headlight.

The proposed radiator was subjected to a thermal analysis, which was conducted using the Solidworks Flow Simulation software (Dassault Systèmes, Vélizy-Villacoublay, France) at an ambient temperature of 26 °C. The LED used in the present study has an on-board multi-LED module with four LEDs on a single board and four chips with a total thermal load of 11.84 W. The thermal resistance (R_{th}) of the LED module was 2.0 °C/W.

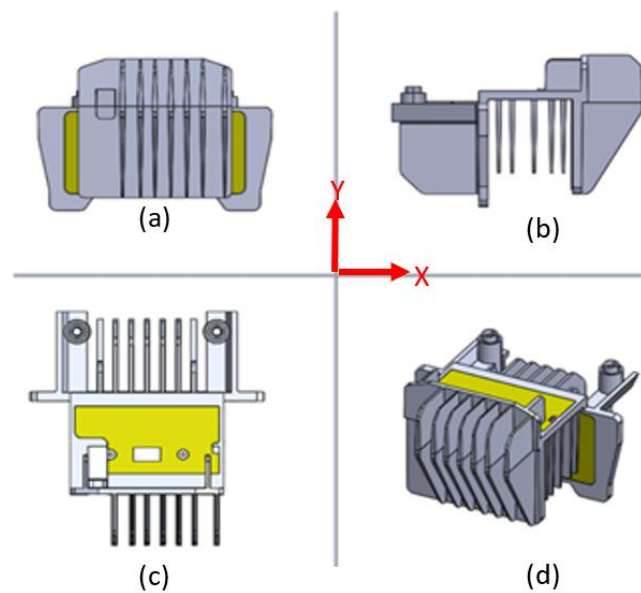


Figure 5. Composite radiator of headlight: (a) front view, (b) side view, (c) top view, and (d) isometric view.

The boundary conditions were set for external flows and included internal space and cavities without flow conditions, a boundary control volume of $1 \times 1 \times 1$ m, and a blackbody wall as the wall radiative surface. Free openings were located on the enclosure boundary, where the model fluid was exposed to the external environment.

Gravity was set to act in the y direction. The grid setting was optimized with respect to the resolution of the walls (a resolution level of 4 was applied).

The temperature T was set to $26\text{ }^\circ\text{C}$ for the surrounding surface. Airflow velocity was set to 0, 0.05, and 0 m/s in the x , y , and z directions. We optimized the length and width of the aluminum alloy and thermally conductive plastic to quickly and evenly conduct heat to the thermally conductive plastic; thereafter, the high emissivity of the thermally conductive plastic ensured the circulation of heat and air, thus achieving heat dissipation while maintaining the low gross weight of the radiator.

Figure 6 shows three temperature points: namely P_1 , representing the pad temperature of the LED module; P_2 , representing the temperature of the mostly aluminum alloy body; and P_3 , representing the temperature on the composite radiator surface. P_1 , P_2 , and P_3 were $60.82\text{ }^\circ\text{C}$, $53.45\text{ }^\circ\text{C}$, and $49.96\text{ }^\circ\text{C}$, respectively. Figure 6a,b present the simulation results of the pure aluminum alloy and the composite radiator for headlights, respectively.

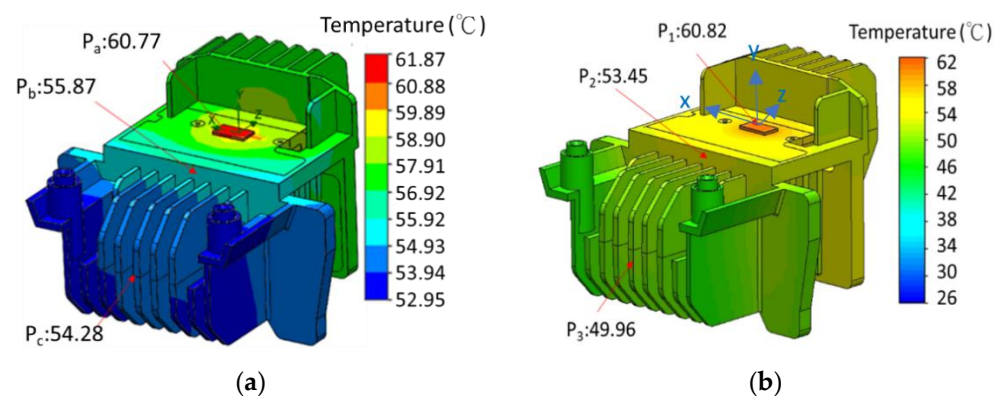


Figure 6. Simulation results for (a) pure aluminum alloy and (b) composite radiator for headlights.

Table 2 summarizes the simulation results at the ambient temperature (T_a) of $26\text{ }^\circ\text{C}$; specifically, it shows the pad temperature of the LED module (P_1), the temperature of the

mostly aluminum alloy body (P_2), and the temperature on the composite radiator surface (P_3). For the aforementioned temperature values, the temperature of the composite heat sink in the LED pad was similar to that of the pure aluminum alloy heat sink.

Table 2. Temperatures of pure aluminum alloy and composite radiators.

Point/Coordinate (x,y,z)	Composite Radiator Temperature (°C)	Pure Aluminum Alloy Temperature (°C)
P_1 (0,0,0)	60.82	60.77
P_2 (0,-2.5,-29.39)	53.45	55.87
P_3 (0,-26.25,-64.35)	49.96	54.28
T_j	66.74	66.69

3. Results and Discussion

Figure 7 depicts the prototype of the composite radiator for headlights, which consists of aluminum alloy and thermoplastic polymer parts. Figure 7a–c present the top, side, and front views, respectively.

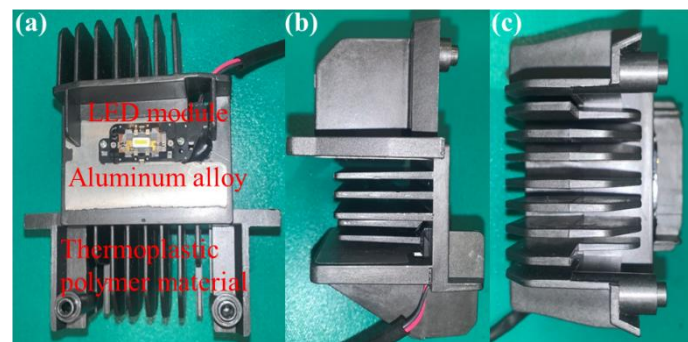


Figure 7. Prototype of composite radiator for headlights: (a) the top view, (b) side view, and (c) front view.

Figure 8 reveals the temperature measurement points on the pad of the LED module (P_1) of the prototype, the temperature measurement points of the mostly aluminum alloy body (P_2), and the temperature measurement points on the composite radiator surface (P_3). We use the TECPEL DTM-317 (TECPEL Co., Ltd. Factory, New Taipei City, Taiwan) to measure the temperature as a thermocouple. At an ambient temperature of 26 °C, the P_1 temperature was 60.8 °C.

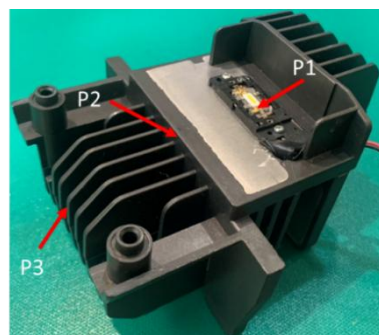


Figure 8. Temperature measurement points on the prototype.

Table 3 presents a comparison of the temperatures obtained through simulation and measurements, and it indicates a high consistency between the simulation and actual

measurements. On the basis of the thermal load and thermal resistance of the LED module, T_j was estimated to be 66.72 °C.

Table 3. Comparison of temperatures obtained through simulation and measurements.

Measured Point	Simulation (°C)	Measured (°C)
The pad temperature of the LED module (P_1)	60.82	60.8
The temperature of the nearly aluminum alloy body (P_2)	53.45	52.8
The temperature on the composite radiator surface (P_3)	49.96	50.5
T_j	66.74	66.72

A temperature measurement time of 0.6 h was required to reach the steady state (Figure 9).

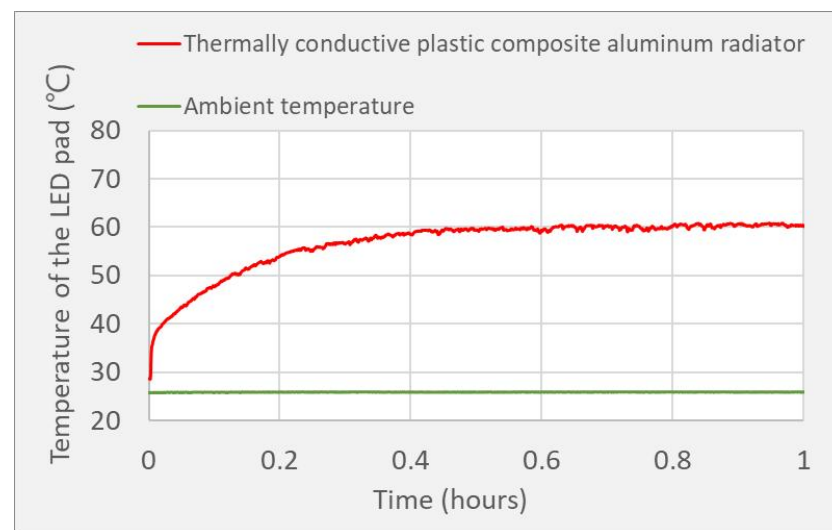


Figure 9. Pad temperature of LED module on composite radiator for headlights.

4. Conclusions

We proposed a lightweight composite headlight radiator that is composed of thermoplastic polymer and insert-molded aluminum alloy parts and designed it for high-power LED headlights, in which it can effectively dissipate heat within a limited space. We optimized the dimensions of the aluminum alloy (AA1050) and thermoplastic polymer to quickly and evenly conduct the heat of the thermally conductive plastic; thereafter, the high emissivity of the thermally conductive plastic ensured the circulation of heat and air, such that heat dissipation was achieved. The prototype composite radiator has an LED module that operates with a thermal load of 11.84 W. The temperature on the LED pad was 60.8 °C, and a low junction temperature T_j of 66.72 °C was achieved. The gross weight of the prototype is 23.37% lower than that of a pure metal radiator. We successfully demonstrated the application of a lightweight, highly insulated composite radiator (for LED headlights) that can meet stringent space, insulation, and weight requirements.

Author Contributions: Z.Y., Y.C., C.H., and J.C. planned the experimental architecture. C.H. and Z.Y. were responsible for simulation data and measurements. Y.C., P.H., J.C., and Z.Y. analyzed the measurement results. C.C. and W.L. wrote the manuscript. Y.C., P.H., J.C., and Z.Y. performed the final article confirmation. All authors have read and agreed to the published version of the manuscript.

Funding: This research was supported by DAYEI PRECISE TECHNOLOGY CO., LTD, PUZI Enterprise CO. LT., and the Ministry of Science and Technology, The Republic of China under the grants MOST 110-2622-E-194-007 and MOST 111-2622-E-005-004.

Institutional Review Board Statement: Not applicable.

Informed Consent Statement: Not applicable.

Data Availability Statement: The data presented in this study are available on request from the first and corresponding authors.

Conflicts of Interest: The authors declare no conflict of interest.

References

1. Katzin, D.; Marcelis, L.F.M.; van Mourik, S. Energy savings in greenhouses by transition from high-pressure sodium to LED lighting. *Appl. Energy* **2020**, *281*, 116019. [CrossRef]
2. Wisniewski, A. Calculations of energy savings using lighting control systems. *Power Syst. Power Electron.* **2020**, *68*, 809–817. [CrossRef]
3. Zhang, H.; Liu, D.F.; Wei, Y.W.; Wang, H. Asymmetric Double Freeform Surface Lens for Integrated LED Automobile Headlamp. *Micromachines* **2021**, *12*, 663. [CrossRef] [PubMed]
4. Wang, H.; Chiang, Y.; Lin, C.; Lu, M.; Lee, M.K.; Feng, S.; Kuo, C. All-reflective RGB LED flashlight design for effective color mixing. *Opt. Express* **2016**, *24*, 4411. [CrossRef] [PubMed]
5. Lua, Z.; Bai, P.; Huang, B.; Henzen, A.; Coehoorn, R.; Liaoe, H.; Zhoua, G. Experimental investigation on the thermal performance of threedimensional vapor chamber for LED automotive headlamps. *Appl. Therm. Eng.* **2019**, *157*, 113478. [CrossRef]
6. Huang, Y.-R.; Chiu, Y.-C.; Huang, K.-C.; Ting, S.-Y.; Chiang, P.-J.; Lai, C.-M.; Jen, C.-P.; Tseng, S.H.; Wang, H.-C. Light extraction efficiency enhancement of flip-chip blue light-emitting diodes by anodic aluminum oxide. *Beilstein J. Nanotechnol.* **2018**, *9*, 1602–1612. [CrossRef]
7. Padmasali, A.N.; Kini, S.G. Accelerated degradation test investigation for life-time performance analysis of LED luminaires. *IEEE Trans. Compon. Packag. Manuf. Technol.* **2020**, *10*, 551–558. [CrossRef]
8. Ye, Z.T.; Chen, C.L.; Chen, L.; Tien, C.H.; Nguyen, H.T.; Wang, H. Hollow light guide module involving mini light-emitting diodes for asymmetric luminous planar illuminators. *Energies* **2019**, *12*, 2755. [CrossRef]
9. Kim, H.Y.; Kim, M.S.; Lee, K.H.; Kang, K.M.; Oh, J.T.; Jeong, H.H.; Seong, T.Y. Optimization of InGaN-based LED package structure for automotive adaptive driving beam headlamp. *ECS J. Solid State Sci. Technol.* **2020**, *9*, 055017. [CrossRef]
10. Ye, Z.T.; Ruan, M.; Kuo, H.C. CSP-LEDs Combined with Light Guide without Reflective Matrix for Antiglare Design. *IEEE Access* **2020**, *8*, 156718–156726. [CrossRef]
11. Ye, Z.; Chang, C.; Juan, M.; Chen, K. Luminous Intensity Field Optimization for Antiglare LED Desk Lamp without Second Optical Element. *Appl. Sci.* **2020**, *10*, 2607. [CrossRef]
12. Qu, X.; Liu, Q.; Blaabjerg, F. System-level lifetime prediction for LED lighting applications considering thermal coupling between LED sources and drivers. *IEEE J. Emerg. Sel. Top. Power Electron.* **2018**, *6*, 1860–1870. [CrossRef]
13. Liu, H.; Yu, D.; Niu, P.; Zhang, Z.; Guo, K.; Wang, D.; Zhang, J.; Ma, X.; Jia, C.; Wu, C. Lifetime prediction of a multi-chip high-power LED light source based on artificial neural networks. *Results Phys.* **2018**, *12*, 361–367. [CrossRef]
14. Qu, X.; Wang, H.; Zhan, X.; Blaabjerg, F.; Chung, H. A lifetime prediction method for LEDs considering real mission. *IEEE Trans. Power Electron.* **2017**, *32*, 8718–8727. [CrossRef]
15. Dumbrava, V.; Pagodinas, D.; Knyva, V.; Kupciunas, I.; Cincikas, G.; Noreika, A.; Siaudinyte, L. Simplified and accelerated method of LED lamp useful life estimation. *MAPAN* **2019**, *34*, 169–178. [CrossRef]
16. Wang, X.; Jing, L.; Wang, Y.; Gao, Q.; Sun, Q. The influence of junction temperature variation of LED on the lifetime estimation during accelerated aging test. *IEEE Access* **2019**, *7*, 4773–4781. [CrossRef]
17. Adhikari, R.; Beyragh, D.; Pahlevani, M.; Wood, D. A numerical and experimental study of a novel heat sink design for natural convection cooling of LED grow lights. *Energies* **2020**, *13*, 4046. [CrossRef]
18. Kilic, M.; Aktas, M.; Sevilgen, G. Thermal assessment of laminar flow liquid cooling blocks for LED circuit boards used in automotive headlight assemblies. *Energies* **2020**, *13*, 1202. [CrossRef]
19. Liu, S.; Wu, J.; Yang, X.; Liu, Y.; Ma, K.; Zhu, H.; Zhou, H.; Sun, H. Analysis of mini-LED light-off phenomenon based on FEM simulation. *Chin. J. Liq. Cryst. Disp.* **2020**, *35*, 53–61. [CrossRef]
20. Huang, Y.; Shen, S.; Li, H.; Gu, Y. Numerical analysis on the thermal performances of different types of fin heat sink for high-power LED lamp cooling. *Therm. Sci.* **2019**, *23*, 625–636. [CrossRef]
21. Ahmed, H.E. Optimization of thermal design of ribbed flat-plate fin heat sink. *Appl. Therm. Eng.* **2016**, *102*, 1422–1432. [CrossRef]
22. Abdelmlek, K.B.; Araoud, Z.; Charrada, K.; Zissis, G. Optimization of the thermal distribution of multi-chip LED package. *Appl. Therm. Eng.* **2017**, *126*, 653–660. [CrossRef]
23. Cenci, M.P.; Berto, F.C.D.; Schneider, E.L.; Veit, H.M. Assessment of LED lamps components and materials for a recycling perspective. *Waste Manag.* **2020**, *107*, 285–293. [CrossRef] [PubMed]
24. Dzombak, R.; Padon, J.; Salsbury, J.; Dillon, H. Assessment of end-of-life design in solid-state lighting. *Environ. Res. Lett.* **2017**, *12*, 084013. [CrossRef]
25. Tang, Y.; Luo, Y.; Du, P.; Wang, H.; Ma, H.; Qin, Y.; Bai, P.; Zhou, G. Experimental investigation on active heat sink with heat pipe assistance for high-power automotive LED headlights. *Case Stud. Therm. Eng.* **2021**, *28*, 101503. [CrossRef]

26. Sevilgen, G.; Kiliç, M.; Aktaş, M. Dual-separated cooling channel performance evaluation for high-power led Pcb in automotive headlight. *Case Stud. Therm. Eng.* **2021**, *25*, 100985. [[CrossRef](#)]
27. Mraz, K.; Bartuli, E.; Kroulikova, T.; Astrouski, I.; Resl, O.; Vancura, J.; Kudelova, T. Case study of liquid cooling of automotive headlights with hollow fiber heat exchanger. *Case Stud. Therm. Eng.* **2021**, *28*, 101689. [[CrossRef](#)]
28. Huang, Y.; Luo, W.; Wang, H.; Feng, S.; Kuo, C.; Lu, C. How smart LEDs lighting benefit color temperature and luminosity transformation. *Energies* **2017**, *10*, 518. [[CrossRef](#)]
29. Lee, C.; Lim, M.; Kim, C.; Bae, S.J. Reliability Analysis of Accelerated Destructive Degradation Testing Data for Bi-Functional DC Motor Systems. *Appl. Sci.* **2021**, *11*, 2537. [[CrossRef](#)]
30. Huang, D.-S.; Chen, T.-C.; Tsai, L.-T.; Lin, M.-T. Design of fins with a grooved heat pipe for dissipation of heat from high-powered automotive LED headlight. *Energy Convers. Manag.* **2019**, *180*, 550–558. [[CrossRef](#)]
31. Mashkov, P.; Gyoch, B.; Ivanovj, R. Investigation of Characteristics and thermal loading of LED bulbs for automatics headlights. *Transp. Probl.* **2018**, *13*, 85–95. [[CrossRef](#)]
32. Ying, S.P.; Chen, B.M.; Fu, H.K.; Yeh, C.Y. Single Headlamp with Low- and High-Beam Light. *Photonics* **2021**, *8*, 32. [[CrossRef](#)]
33. Zhu, Z.; Wei, S.; Liu, R.; Hong, Z.; Zheng, Z.; Fan, Z.; Ma, D. Freeform surface design for high-efficient LED low-beam headlamp lens. *Opt. Commun.* **2020**, *477*, 126269. [[CrossRef](#)]
34. Chu, S.-C.; Chen, P.-Y.; Huang, C.-Y.; Chang, K.-C. Design of a high-efficiency LED low-beam headlamp using Olikier's compound ellipsoidal reflector. *Appl. Opt.* **2020**, *59*, 4872–4879. [[CrossRef](#)] [[PubMed](#)]
35. Ma, S.-H.; Lee, C.-H.; Yang, C.-H. Achromatic LED-based projection lens design for automobile headlamp. *Optik* **2019**, *191*, 89–99. [[CrossRef](#)]
36. Cavallo, V.; Espie, S.; Dang, N.T. Improving motorcycle motion perception by using innovative motorcycle headlight configurations: Evidence from simulator and test-track experiments. *Accid. Anal. Prev.* **2021**, *157*, 106118. [[CrossRef](#)]
37. You, Z.; Yang, D.; Zhou, P.; Hai, Y.; Liu, D.; Hou, F. Heat transfer analysis of vapor chamber heat pipe for high power LED package. In Proceedings of the 2010 11th International Conference on Electronic Packaging Technology & High Density Packaging, Xi'an, China, 16–19 August 2010. [[CrossRef](#)]
38. Yu, G.-Y.; Zhu, Z.-P.; Hu, S.-H.; Hao, W.-W.; Guo, T.-T. Thermal simulation and optimization design on a high-power LED spot lamp. *Optoelectron. Lett.* **2011**, *7*, 117–121. [[CrossRef](#)]
39. Tang, Y.; Liu, D.; Yang, H.; Yang, P. Thermal effects on LED lamp with different thermal interface materials. *IEEE Trans. Electron Devices* **2016**, *63*, 4819–4824. [[CrossRef](#)]
40. Park, D.H.; Lee, D.B.; Seo, E.R.; Park, Y.J. A parametric study on heat dissipation from a LED-lamp. *Appl. Therm. Eng.* **2016**, *108*, 1261–1267. [[CrossRef](#)]